Available online at www.sciencedirect.com
ScienceDirect
Optics & Laser Technology 40 (2008) 405–414
Optics & Laser Technology
www.elsevier.com/locate/optlastec

Surface nitriding of Ti–6Al–4V alloy with a high power CO_2 laser

J.H. Abboud[a], A.F. Fidel[b], K.Y. Benyounis[c,*]

[a]Department of Mechanical Engineering, Faculty of Engineering, Garyounis University, P.O. Box 1308, Benghazi, Libya
[b]Department of Mechanical Engineering, Omar Al-Mukhtar University, Al-bythaa, Libya
[c]Department of Industrial Engineering, Faculty of Engineering, Garyounis University, P.O. Box 1308, Benghazi, Libya

Received 30 March 2007; received in revised form 12 July 2007; accepted 15 July 2007
Available online 10 September 2007

Abstract

Surface nitriding of a Ti–6Al–4V alloy by laser melting in a flow of nitrogen gas has been investigated, with the aim of increasing surface hardness and hence improving related properties such as wear and erosion resistance. The effect of the scanning speed, nitrogen dilution, and nitrogen flow rate on microstructure, microhardness, and cracking of the nitrided layers was studied. Optical, scanning electron microscopy, energy dispersive spectroscopy, and X-ray diffraction (XRD) were used to reveal the microstructure and to identify the phases formed. It is shown that smooth, deep, and crack-free nitride layers of a surface hardness ranging between 500 and 800 HV can be obtained by controlling the processing parameters. Cracks are present in the sample processed at slow scanning speed and high laser power. Dilution of the nitrogen gas with argon gas leads to a crack-free nitride layer at the expense of a reduction in surface hardness. Slow scanning speeds lead to the formation of a deep and hard surface layer, and increasing the nitrogen flow rate results in a rough surface with a slight increase in hardness.

Keywords: Laser surface nitriding; Ti–6Al–4V; XRD

1. Introduction

Ti–6Al–4V alloys exhibit a remarkable combination of high specific strength and good oxidation resistance, which make them useful for high-temperature applications [1]. However, they suffer from low wear resistance, which limits them in applications where abrasive or erosion phenomena are present. The formation of TiN on the surface of titanium and its alloys is the most popular way to improve their corrosion and wear properties. Solid-state nitriding by chemical vapour deposition (CVD), plasma nitriding and physical vapour deposition (PVD) is widely used for this purpose. All of these methods have their drawbacks, such as the need for the whole work piece to be heated, and that the coatings are formed over all surface and are brittle. Another disadvantage is the depth of coating or hardening, which is restricted by low diffusivity [2,3]. This problem can be addressed by laser nitriding the titanium surface in the molten state.

Laser nitriding is generally obtained by a reaction between a laser molten top layer and nitrogen producing nitrides, which after solidification become a hard composite layer with low friction coefficient. The technique of laser nitriding was initiated by the work of Katayama et al. [4] and since then there have been a number of such investigations [5–15]. The structure of the nitrided layer is very dependent upon processing conditions but the matrix is generally constituted from fine nitride needles [12] or dendrites [9] embedded in a nitrogen-rich titanium matrix. The substrate in contact with the molten layer is composed of the martensite type α'-titanium structure formed during rapid cooling. Laser nitriding on commercial purity titanium (CP) produced high surface hardness values, in excess of 2000 HV, with a hardness of at least 1000 HV retained to a depth below the surface of 0.4 mm [8].

The presence of microcracks is reported as a major problem associated with laser gas nitrided layers of

*Corresponding author.
E-mail addresses: jhabboud@yahoo.com (J.H. Abboud), elmhdi772000@yahoo.com (A.F. Fidel), kybenyounis@yahoo.com (K.Y. Benyounis).

0030-3992/$ - see front matter © 2007 Elsevier Ltd. All rights reserved.
doi:10.1016/j.optlastec.2007.07.005

titanium alloys [8], although crack-free nitrided layers were obtained using pre-heated sample [10] or by diluting nitrogen gas with argon [11], but at the expense of a reduction in surface hardness. In this regard, it is relevant to mention that it is essential to optimise the laser and the process parameters to avoid the formation of cracks and to form a defect free and continuous surface layer.

In the present study, an attempt has been made to undertake laser nitriding of Ti–6Al–4V alloy using a continuous wave CO_2 laser. The effect of laser parameters on the microstructure, phases, microcracks, and microhardness has been studied in detail.

2. Experimental techniques

2.1. Material and sample preparation

The material used in this study is Ti–6Al–4V alloy of 3 mm thickness. The specimens were cut in the form of plates ($10 \times 10 \times 3$ mm) using wire electrical discharge cutting machine. Before laser nitriding, the surface of the samples were abraded with 600 grit SiC papers, and then cleaned ultrasonically with methanol. The initial non-irradiated roughness is about 2–3 μm.

2.2. Laser gas nitriding

The laser used in this investigation is a CO_2 laser operating in both continuous and pulse mode. The output power is 3 kW. The laser beam is focused by a ZnSe lens with a focal length of 200 mm. The minimum diameter of the focused beam is ~0.5 mm. The relative movement between laser beam and work piece is realised by a computer numerical controlled (CNC) X–Y–Z nozzle. For alignment procedures, a HeNe laser beam was transmitted along the optical axes.

The experimental set-up of a laser gas nitriding process is illustrated schematically in Fig. 1. The laser beam is reflected by mirror toward the specimen and is focused by the lens to a point approximately 10 mm below the nozzle and 10–15 mm above the specimen surface. Because of the high affinity of titanium to oxygen, titanium nitriding by laser requires an efficient shroud to prevent oxidation. A gas shielding device is made to serve three purposes; firstly to prevent oxidation, secondly to supply the nitrogen gas to the melted zone, and thirdly to push away the plasma which forms above the melted zone. The formation of the plasma prevents the absorption of the laser beam and in some instances it causes the lens to break. Fig. 2 shows the attachment of the shroud system to the laser head. The distance between the shielding device and sample was kept very small ~1 mm to prevent air from entering the laser-melted zone.

The flow rate of nitrogen gas was controlled using two calibrated flow metres: one for nitrogen and other for argon. The axial nozzle is used to supply the nitrogen atmosphere. Side flow is necessary to prevent plasma formation and the suck in of oxygen. All nozzle diameters amount to at least several times the melt pool diameter. In order to prevent mixing with air, the gas flow must never become turbulent. The specimen was fixed on the table by putting it into the holder to prevent movement during the process.

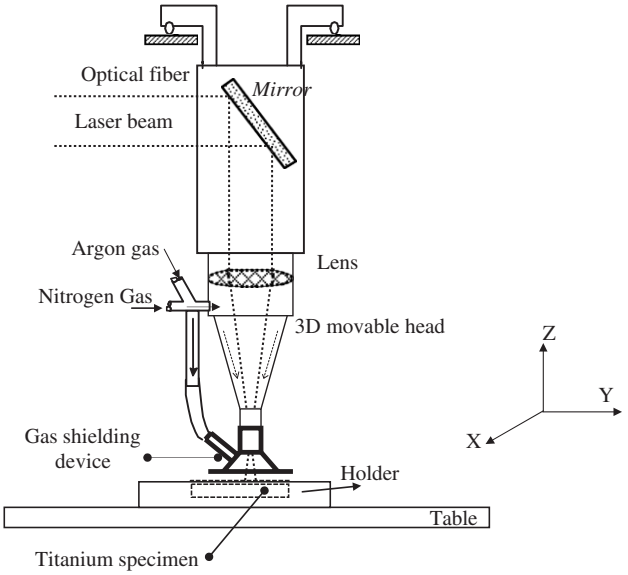

Fig. 1. A schematic diagram of the laser nitriding experimental set-up.

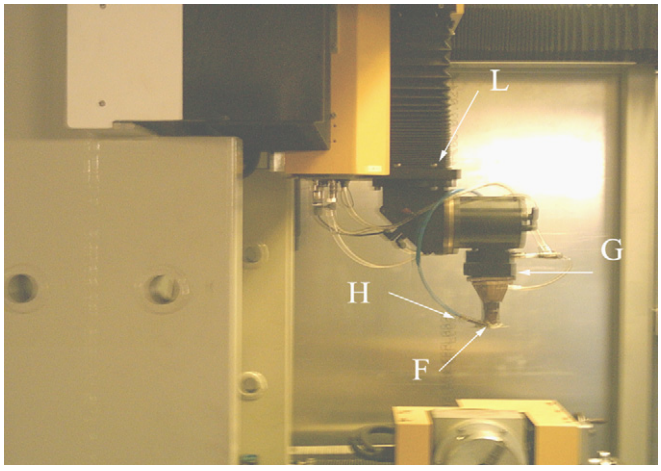

Fig. 2. Photographs showing the assembly of shrouding system with head of laser: F, shrouding device; H, side nozzle; G, laser head; and L, laser mirror.

2.3. Surface characterisation method

Microstructural characterisation and microanalysis was carried out on transverse sections using optical microscopy, scanning electron microscopy (SEM) and X-ray energy dispersive spectrometry (EDS). Specimens were etched with a reagent consisting of 5 ml HF and 5 ml HNO_3 in 85 ml of water. A scanning electron microscope model

LEO1430 VP, using LaB_6 filament, is used. For X-ray diffraction (XRD), surface layers are produced by overlapping of single melt typically by about 40%. The width of the overlapped layers was 15 mm which is sufficient for this test. A D5005 diffractometer employing Cr Kα radiation was used for structural analysis of the different phases and compounds formed. The X-ray device is equipped with a software contain d-spacings of all compounds including titanium and TiN. Microhardness measurements were taken mainly on transverse sections using a Shimaduz microhardness tester and a 100 g load.

3. Results and discussions

3.1. The microstructure and microhardness

The nitrided layer was produced using laser power of 2.5 kW, a 15 mm focal length lens, a laser scanning speed of 900 mm/min, in a 100% nitrogen environment, and a flow rate of 1000 l/h. The nitrided layer showed a golden colour and a relatively rough surface. At some places perpendicular cracks and microcracks running parallel to the surface were observed. The relationship between the crack intensity and the processing parameters will be discussed

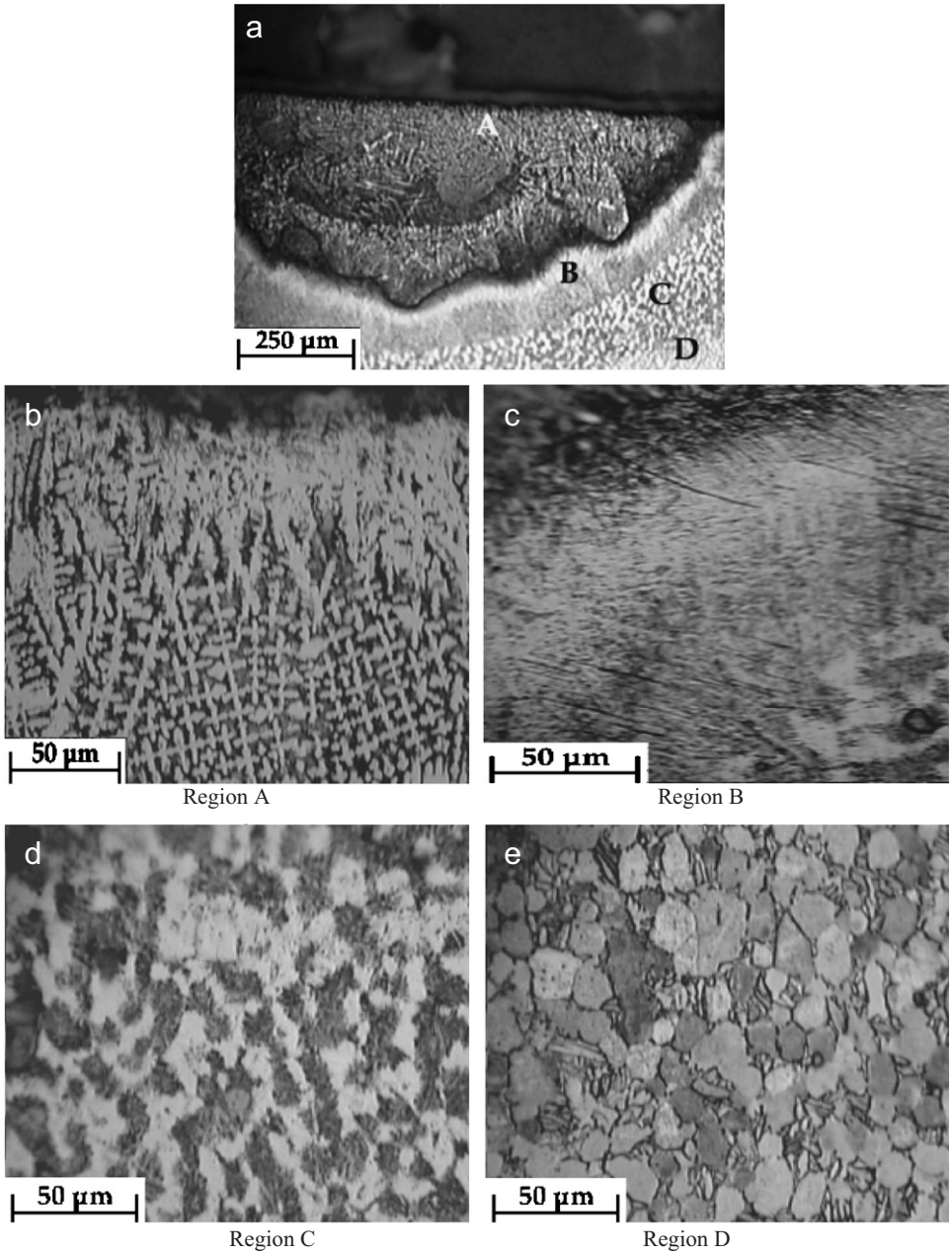

Fig. 3. Optical micrographs of cross-section of laser nitride layer of Ti–6Al–4V ($P = 2.5$ kW, $V = 900$ mm/min, flow rate = 1000 l/h, 100% N_2). (a) The whole layer at low magnification and (b–e) each region at higher magnification.

later. A transverse section is shown in Fig. 3. The nitrided layer is 0.45 mm thick. Dendrites were observed in the nitrided layer; Fig. 3a. The dendrites in the top of the layer were oriented perpendicular to the surface while below the surface they were randomly distributed and decreased with distance from the surface (Fig. 3b). The lower part of the nitrided layer shows a mixture of dendrites and needle shaped phase. Below the fusion zone, there is the heat-affected zone (HAZ) (region B in Fig. 3a). This region showed only needle-shaped structure, resembling titanium martensite. Fig. 3c shows the partially transformed structure while Fig. 3d shows the structure of the unaffected substrate, which is a mixture of α and a small amount of β.

SEM examination of the nitride layer reveals the morphology and the size of these dendrites in detail. The primary dendrites are ~10 μm long and 2–3 μm in width. The secondary dendrites originated from the primary dendrite. The dendrite arm spacing as measured from the SEM micrograph was less than 2 μm. The top section of the nitride layer shows more clearly the rippling effect and columnar grain-oriented parallel to the scanning speed. This ripple affects the surface roughness. It has been shown that temperature gradients between the centre and the edge of fusion zone lead to surface tension gradients. The minimum surface tension will be in the centre (maximum temperature) and maximum surface tension will be in the edge. This in turn leads to fluid flow. The consequence of fluid flow is the roughening of the surface. The effect of processing parameters, such as scanning speed, laser power, and nitrogen flow rate will be presented later.

A nitrogen concentration gradient is expected to exist because the solution of the gaseous nitrogen is temperature and time dependent. Previous work of EDS analysis on CP Ti [15] has shown a 30 at% N near the surface decreased across the layer thickness reaching 0% in the lower part of the layer. In the present work, EDS analysis of area (5 μm × 5 μm) in the nitride layer was carried out. The nitrogen concentration in the dendrite (~30 at%, region B in Fig. 4) indicates that it may be TiN, while in the needle like structure it had a low concentration of about 10 at% (region A in Fig. 4).

The microhardness profile across the nitrided layer is shown in Fig. 5. The graph indicates that the maximum hardness of about 1350 HV extended to a shallow depth 50–80 μm below the surface for nitrided layer produced with laser power 2.5 kW, nitrogen flow rate of 1000 l/min, and scanning rate of 900 mm/min. The microhardness then decreased to 800 HV and extended for a depth 0.4 mm below the surface. The dense dendrite regions in the nitrided layer produced a greater hardness compared with other regions with lower concentrations. The high hardness near the surface is attributed to the high concentration of nitrogen in the surface. Several other studies have shown that the hardness increases with increasing concentration of TiN in the nitrided layer [4,5,8].

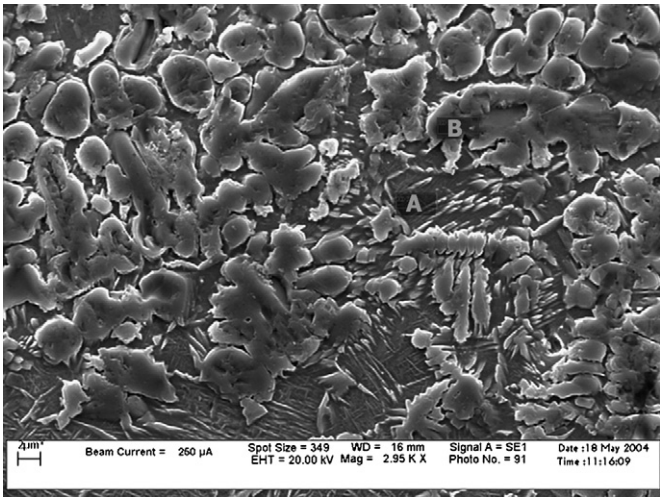

Fig. 4. SEM micrograph using back scattered electron showing the microstructure of the nitrided layer.

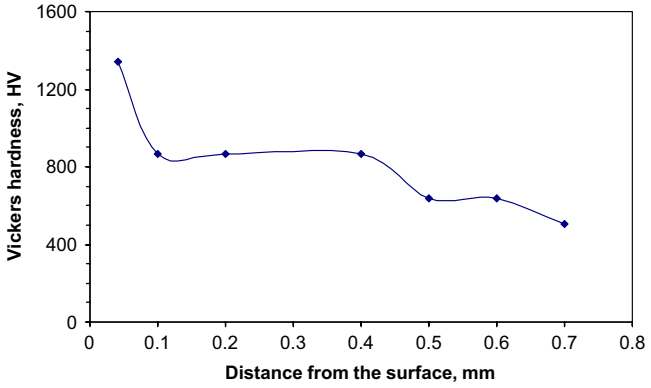

Fig. 5. Hardness profile across the nitrided layer processed using a laser power of 2.5 kW and scan rate of 900 mm/min.

3.2. X-ray diffraction

The possible phases formed in the nitrided layer are dependent on the laser processing conditions used, such as nitrogen concentration, laser power density, and traverse speed. They also varied with the depth and location in the nitrided layer. In the present investigation, most of the nitrided layers showed a dendritic structure in a matrix of needle-shaped phase (see Figs. 3b and 4). The dendrites were concentrated at the surface and extended to a depth of 0.25 mm. In order to determine the phases present in the nitrided layer, the X-ray spectrum was obtained from the surface of nitrided sample processed at (2.5 kW, 900 mm/min, 100% N_2). The nitrided layer produced by overlapping technique-covering area of 15 mm wide. The X-ray spectrum in Fig. 6 shows that two phases, mainly TiN and α'-Ti, were formed on the surface. It is noted that the intensity of the TiN peaks appeared much stronger than that of the α'-Ti peaks. By referring to Figs. 3b and 4, a conclusion can be drawn that the dendrites are TiN and

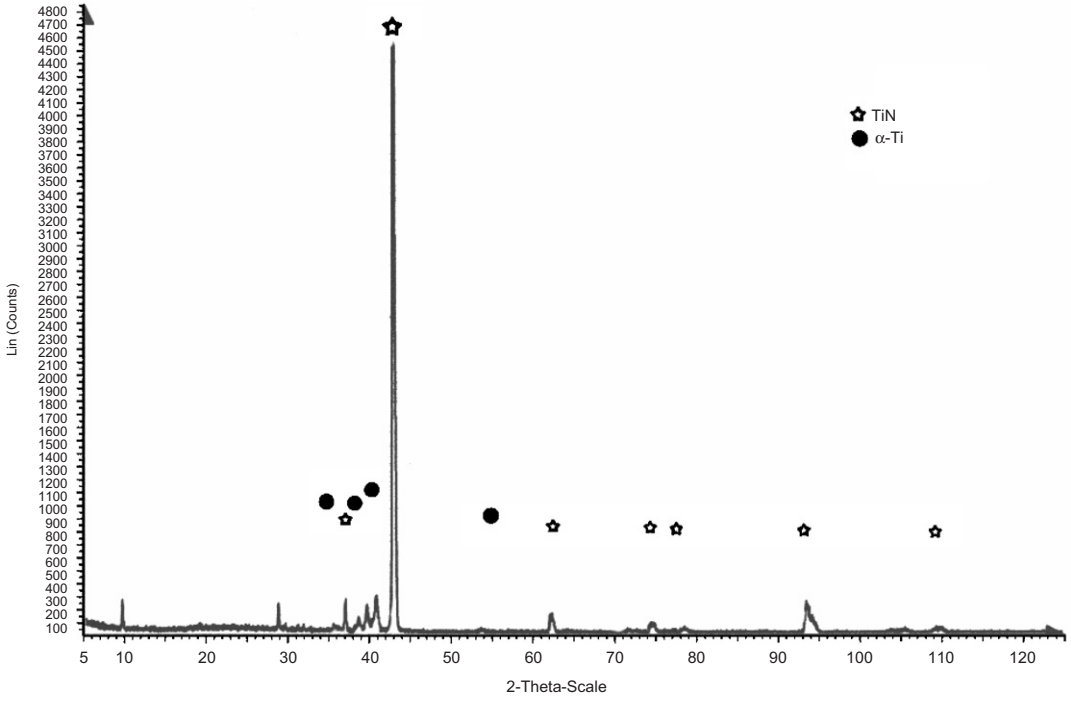

Fig. 6. XRD pattern of the nitrided layer.

between the dendrites is α′-Ti. This result agreed with the work of Baker and co-workers [11] who study in detail the phases present in the nitrided layer of the same alloy produced by laser and also with many investigators who study laser nitriding of Ti–6Al–4V alloy [6–8].

3.3. Effect of the processing parameters

3.3.1. Nitriding with different scanning speeds

Fig. 7 shows transverse sections of the nitride layer produced at different scanning speeds. The size of nitride layer was decreased when the speed was increased. This is due to the reduction of the interaction time between the laser beam and the specimen. Fig. 8 shows the microhardness of a laser-treated titanium specimen as a function of the depth from the surface of the specimen down to 800 μm. The maximum surface microhardness was over 750 HV. A slower laser traverse speed resulted in a slight increase in the microhardness. The hardness level in the alloyed layer is determined principally by the traverse speed and by the laser power. From an economics point of view of the process and the prevention of the formation of defects, such as cracks and pores, the scanning speed should be as high as possible. However, a high traverse speed usually leads to insufficient hardening and to inhomogeneity in the resulted layer, and a certain reaction time is required in order to achieve the necessary hardness and melt depth. The scatter and sharp drop in the hardness values, which is frequently observed in most of the nitrided layers, is attributed to convectional loops, which push the dendrite a way from the centre to the edge.

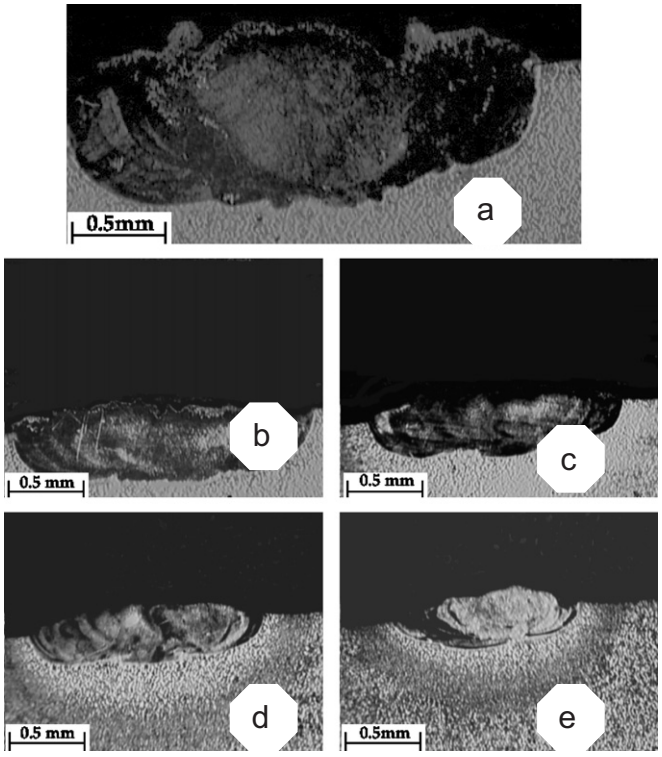

Fig. 7. Optical micrograph showing the cross-section of laser tracks of Ti–6AL–4V at different traverse speeds (*V*): (a) 300 mm/min, (b) 500 mm/min, (c) 800 mm/min, (d) 1000 mm/min, and (e) 1500 mm/min.

3.3.2. Nitriding with diluted nitrogen

Fig. 9a–d shows sections profiles of the nitrided layers which were produced with increasing the amounts of

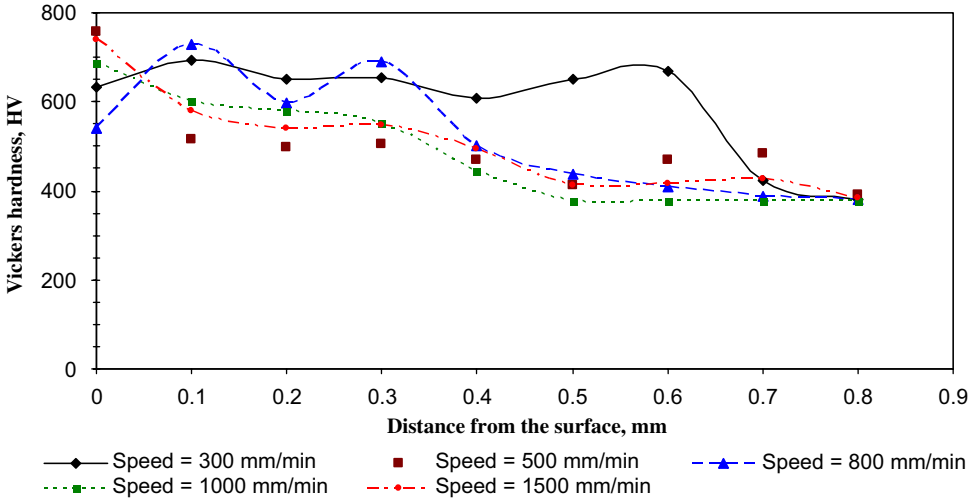

Fig. 8. Microhardness profile across the nitride layers produced at different scanning speeds.

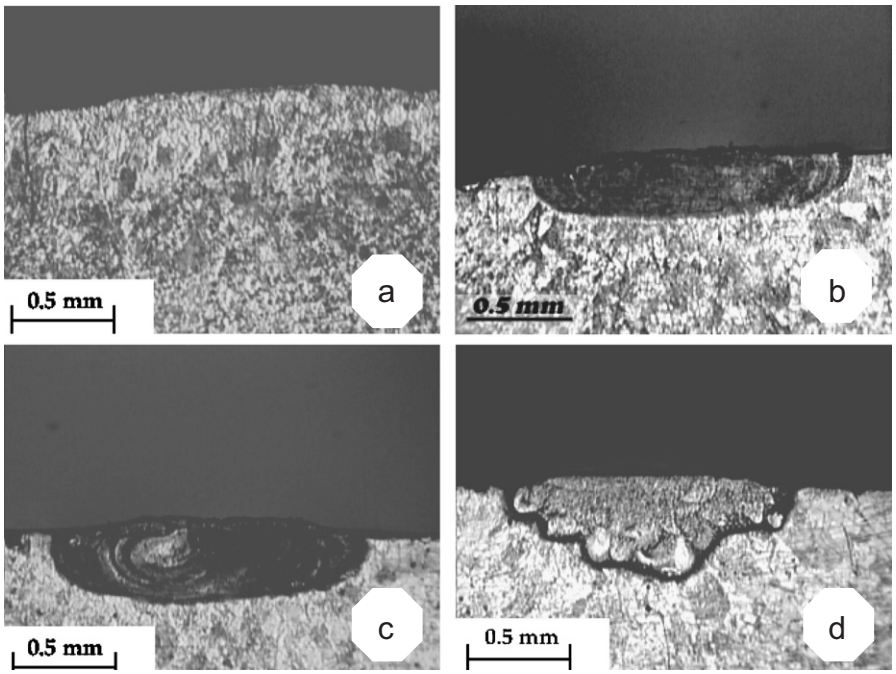

Fig. 9. Optical graphs of nitrided layers at different nitrogen content in the nitrogen/argon gas mixture: (a) 0% N_2, (b) 40% N_2, (c) 60% N_2, and (d) 100% N_2.

nitrogen mixed with argon. The shape of the nitrided layer is strongly affected by the increase of the nitrogen content. The processed layer using 0% nitrogen or 100% argon showed a silver colour surface and only a martensitic structure as shown in Fig. 9a. But, as the nitrogen concentration is increased as in Fig. 9b and c, the alloyed layer becomes wider and flat-bottomed with no cracks. No dendrites were observed in the nitrided layer processed at 40% and 60% nitrogen; a continuous film (~1 μm) assumed to be TiN was observed on the surface on the specimen processed at 60% nitrogen. As the amount of nitrogen increased towards 100%, the shape of the alloyed layer become deeper and the interface become irregular; also the surface colour become more golden as the amount of nitrogen mixed increased; Fig. 9d. This is attributed to the exothermic heat of solution and convection fluid flow [10]. Microhardness measurements across these layers indicate that a lower hardness at the surface was developed in the nitride layer using lower nitrogen concentration, Fig. 10. These nitrogen concentration conditions actually decrease the dissolution of nitrogen, and the subsequent concentration of TiN dendrites in the melt at the surface, resulting in lower hardness values. The specimen processed at pure nitrogen show a maximum hardness of more than 1000 HV extended to a depth of 150 μm below the surface; this can be attributed to the TiN dendrites which are

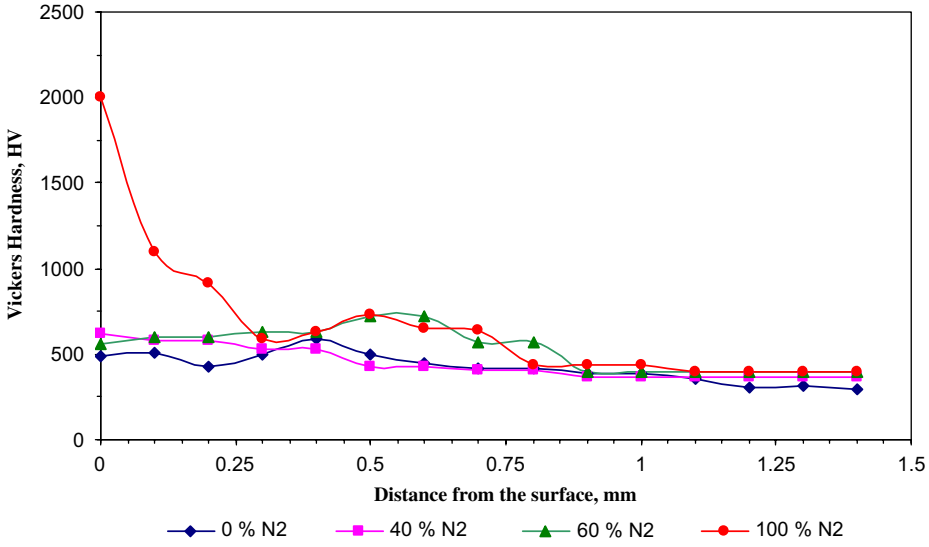

Fig. 10. Microhardness profile across the nitride layer produced on Ti–6Al–4V at different nitrogen concentrations.

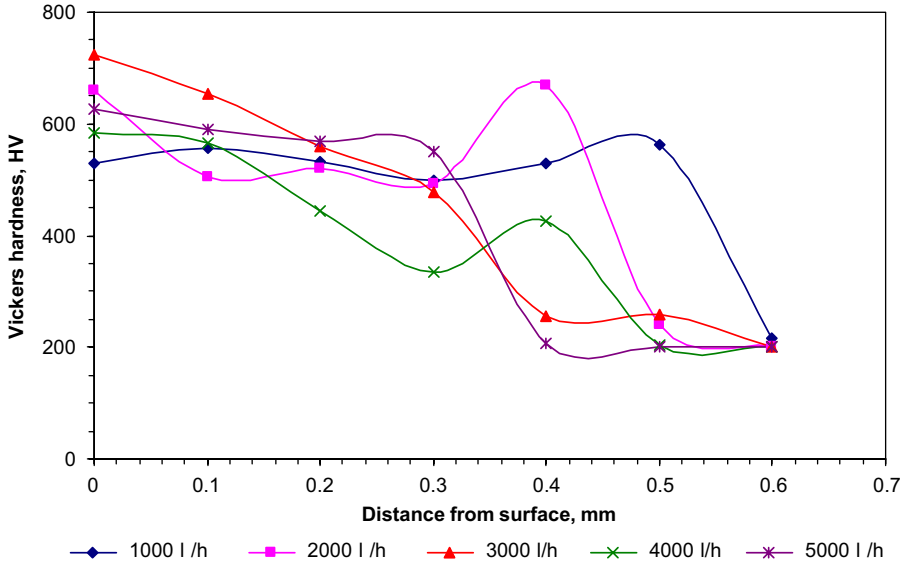

Fig. 11. Microhardness profile across the nitride layer produced at different gas flow rates.

concentrated at and below the surface. The specimen produced with diluted nitrogen having no TiN dendrites; the thickness of these layers was typically 0.3 mm and the hardness ranged between 400 and 500 HV.

3.3.3. *Nitriding with different nitrogen gas flow rates*

The microhardness is plotted against melt depths for a series of nitrided layers produced at different nitrogen gas flow rates as shown in Fig. 11. The graphs indicate that a lower hardness at the surface was developed in the nitride layer using lower nitrogen flow rates (1000 l/h). These gas flow rates and specimen velocity conditions actually decreased the dissolution of nitrogen, and the subsequent concentration of TiN dendrites in the melt at the surface, resulting in lower hardness values. The graphs also give shallow hardness profiles over a 0.50 mm depth for tracks produced with higher flow rate (5000, 4000, and 3000 l/h). The maximum hardness developed was about 724 HV for tracks produced with a 3000 l/h gas flow rate, which is over two times higher than the base hardness 350 HV. Laser nitriding at a low nitrogen flow rate reduced the availability of nitrogen for dissolution in the melt, and hence fewer nitride nucleation sites were believed to be present.

The overall view of the results which contain experimental parameters as scanning speed, nitrogen flow rate, and nitrogen concentration in gas as well as microhardness values at 0.2 mm below the surface are presented in Table 1. These results showed a maximum hardness can be obtained at slow speed, moderate flow rate and using

Table 1
Laser processing parameters used in this investigation (2.5 kW laser power)

Specimen no.	Track no.	Scanning speed (mm/min)	Flow rate (l/h)	Nitrogen concentration (%)	Hardness (HV) at 0.2 mm below the surface
1	A-1	300	1000	100	650
	A-2	500	1000	100	500
	A-3	800	1000	100	600
	A-4	1000	1000	100	590
	A-5	1500	1000	100	550
2	B-1	1000	1000	100	850
	B-2	1000	1000	60	525
	B-3	1000	1000	40	520
	B-4	1000	1000	0	400
3	C-1	900	1000	100	585
	C-2	900	2000	100	580
	C-3	900	3000	100	500
	C-4	900	4000	100	500
	C-5	900	5000	100	450

100 N_2. Also, it is very clear that dilution of nitrogen with argon lead to a decrease in the hardness.

3.4. Surface morphology and cracking

Generally, laser treatment of material induces tensile stresses in the material. In the case of a metal, these stresses can be relieved by elastic and plastic deformation. However, ceramic material shows more brittle behaviour and laser treatment may cause cracking [6]. In these experiments, cracks in the laser tracks indicated the build up of a tensile stress in the scan direction, which will be released by perpendicular cracking if it is exceed a critical stress as can be seen in Fig. 12.

For a single laser tracks, crack formation in the scan direction only occur for very high laser energy densities. However, for overlapping tracks cracking occur in the scan direction, which can be explained by an increase in the residual stress with each successive overlapping laser track up to maximum value.

In the present work, all the treated samples were examined by optical microscope for cracks existing in the nitride layer, its growth within the nitride layer in two-dimensional namely traverse section and longitudinal section. The results revealed that the main parameters controlling of cracks are the nitrogen concentration in the environments and power density, while the scanning velocity has a significant effect on the shape and morphology.

For different scan velocities, the shape of the melt pool and solidification front changes, as shown in Fig. 13. The surface rippling and the in homogeneity in the as-formed layer are attributed to surface tension driven fluid flow. Surface tension gradients are set up by temperature gradients and appear to be much enhanced by nitrogen concentration gradients on the melt pool surface. Nitrogen

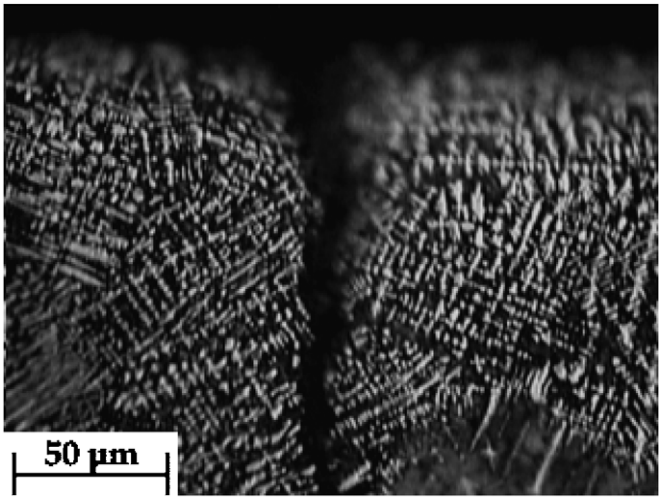

Fig. 12. Top view showing crack in some of the processed layer.

concentration gradients are expected to exist because the solution of the gaseous nitrogen is temperature and time dependent. In fact, the melt pool is elongated and extends beyond the beam diameter in the longitudinal direction. The surface morphology of a laser nitride layer with a traverse speed of 300 mm/min showed a relatively flat surface with some ripples is formed as can be seen in Fig. 13a. With traverse speed of 500 mm/min the ripples, features become significant as shown in Fig. 13b. With further increase in the speed to 800 mm/min, a rippled surface is formed as it can be seen in Fig. 13c. At traverse speed 1500 mm/min, predominant epitaxial features are observed on the nitride surface as shown in Fig. 13d.

A change in nitrogen concentration affected the surface roughness and cracking severity. With a nitrogen concentration of 100% N_2, the surface is rough with a golden colour; cracks were observed as shown in Fig. 14a. When the nitrogen concentration was decreased to 60%, the nitride surface became relatively smoother with small cracks were formed. A further decrease in the nitrogen concentration to 50% produced comparatively a smooth surface with cracks free. When the nitrogen is stopped (only argon is flow), the melted zone is very smooth and flat surface with a silver colour.

4. Conclusions

Surface nitriding of Ti–6Al–4V can be achieved by laser melting in a flow of nitrogen gas, and high surface hardness values, in excess of 1000 HV could be achieved. Also, the hardness and the hardening depth depend greatly on the volume fraction of TiN formed during solidification. It has been found that slow scanning speed, high power density and relatively high flow rate could lead to a high surface hardness up to a depth of 0.5–0.8 mm. Although the surface hardness could be decreased, the cracks intensity can be significantly reduced by mixing the nitrogen with argon gas. The microstructure of the nitrided layer is

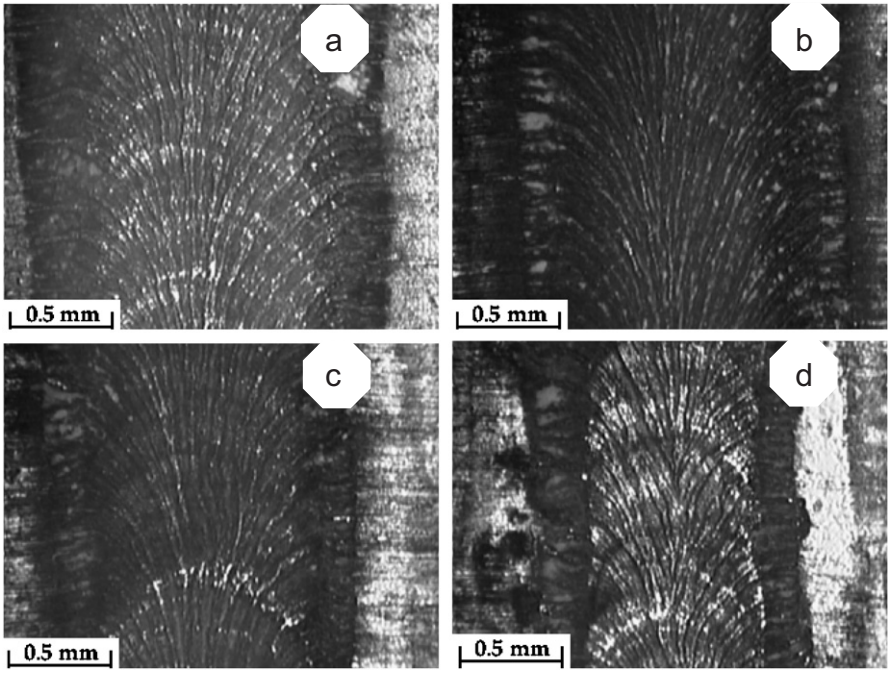

Fig. 13. Top view of the laser nitrided layer produced at different scanning speeds: (a) 300 mm/min, (b) 500 mm/min, (c) 800 mm/min, and (d) 1500 mm/min.

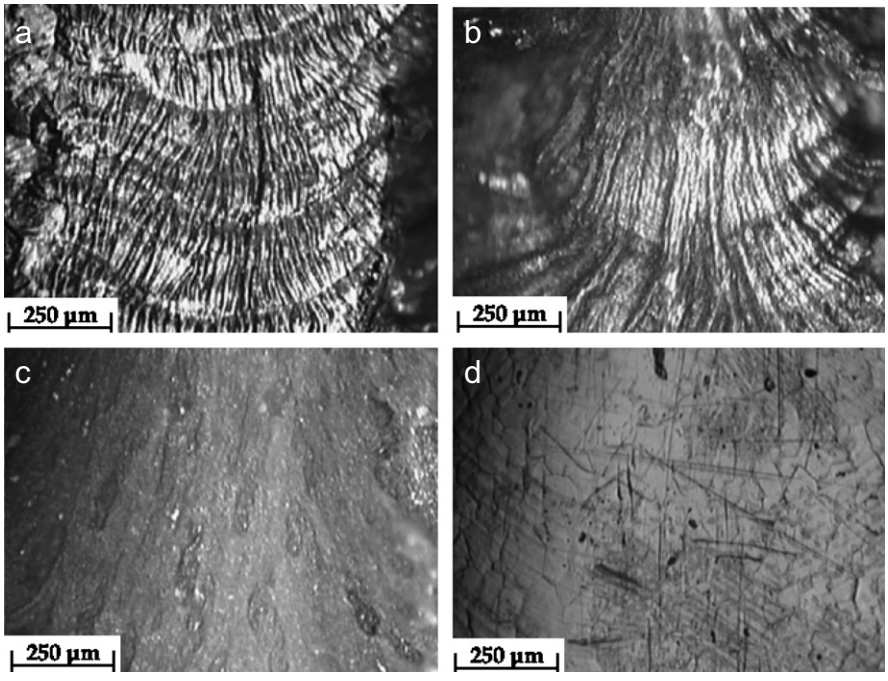

Fig. 14. Top view of the processed layer at different nitrogen concentration: (a) 100% N_2, (b) 60% N_2, (c) 50% N_2, and (d) 0% N_2.

dendritic, however, cracks have been observed specially in the nitride layers processed at slow speed and high power. From the characterisation results, it was found that solidified melt consists of TiN dendrites and α'-Ti. Generally, increasing the scanning speed would decrease the crack intensity and also decrease the thickness of the nitrided layer formed.

Acknowledgements

The authors wish to thank laser research centre in Tripoli for their help in using the laser, to petroleum research centre specially Osama Burshan for using the SEM and to Dr. Mohammed A. Alalam in industrial research centre for the use of XRD and microhardness tester.

References

[1] Polmear J. ''Light alloys,'' metallurgy of the light metals. London: Arnold; 1995.
[2] Miller PD, Holladay JW. Friction and wear properties of titanium. Wear 1958/59;2.
[3] Kenneth GB. Tribological properties of titanium alloys. Wear 1991;151:203–17.
[4] Katayama S, Matsunawa A, Morimoto A, Ishimoto S, Arata Y. Surface hardening of titanium by laser nitriding. In: ICALEO'83 LIA, Los Angeles, 1983. p. 5.
[5] Mordike BL. Laser gas alloying. In: Draper CW, Mazzoldi P, editors. Laser surface treatment of metals. Dordrecht: Kluwer; 1986. p. 389–413.
[6] Kloosterman AB, De Hosson JThM. Microstructural characterization of laser nitrided titanium. Scr Metall Mater 1995;33(4):567–73.
[7] Bell T, Bergmann HW, Lanangan J, Staines AM, Morton PH. Surface engineering of titanium with nitrogen. Surf Eng 1986;2: 133–43.
[8] Mridha S, Baker TN. Effects of nitrogen gas flow rates on the microstructure and properties of laser-nitrided IMI318 titanium alloy (Ti–6A1–4V). J Mater Process Technol 1998;77:115–21.
[9] Kloosterman AB, De Hosson JM. Surface modification of titanium with lasers. PhD thesis, University of Groningen, The Netherlands, 1998.
[10] Weerasinghe VM, West DRF, Czajlik M. Laser surface nitriding of titanium and a titanium alloy. In: Proceedings of the first ASM conference on heat treatment and surface engineering, Amsterdam, 1991.
[11] Selamat MS, Baker TN, Watson LM. Study of the surface layer formed by the laser processing of Ti–6A1–4V Alloy in a dilute nitrogen environment. J Mater Process Technol 2001;113:509–15.
[12] Nwobu P, Rawlings RD, West DRF. Nitride formation in titanium based substrates during laser surface melting in nitrogen–argon atmospheres. Acta Mater 1999;47(2):631–43.
[13] Weerasinghe VM, Westb DRF, de Damborenea J. Laser surface nitriding of titanium and a titanium alloy. J Mater Process Technol 1996;58:79–86.
[14] György A, Pérez del Pino P, Serra JL, Morenza A. Influence of the ambient gas in laser structuring of the titanium surface. J Surf Coat Technol 2004;187:245–9.
[15] Fidel AF. Surface hardening of titanium with laser. MSc thesis, Department of Mechanical Engineering, University of Garyounis, Benghazi, Libya, 2004.